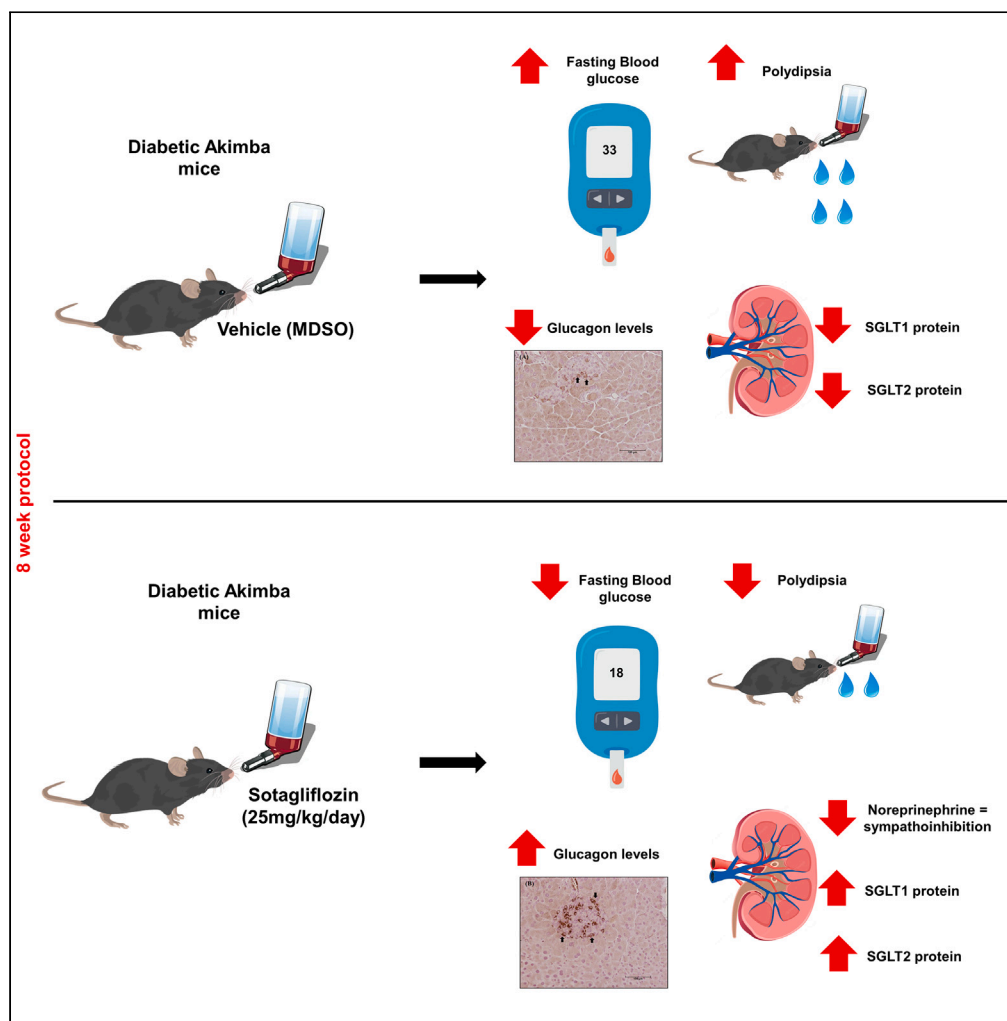# iScience

Article

SGLT1/2 inhibition improves glycemic control and multi-organ protection in type 1 diabetes

Lakshini Yasaswi
Herat, Jennifer
Rose Matthews,
Moira Hibbs,
Elizabeth Piroska
Rakoczy, Markus
Peter Schlaich,
Vance Bruce
Matthews

vance.matthews@uwa.edu.au

Highlights

Dual SGLT1/2 inhibition
promoted compensation
of renal SGLT1/SGLT2
protein levels

Sotagliflozin significantly
increased pancreatic islet
glucagon protein
expression

Sotagliflozin reduced
sympathetic nerve
activation in diabetic
Akimba mice

Sotagliflozin treatment
prevented deaths
associated with diabetes
in Akimba mice

Article

SGLT1/2 inhibition improves glycemic control and multi-organ protection in type 1 diabetes

Lakshini Yasaswi Herat,[1,6] Jennifer Rose Matthews,[1,6] Moira Hibbs,[2] Elizabeth Piroska Rakoczy,[3] Markus Peter Schlaich,[4,5,7] and Vance Bruce Matthews[1,7,8,*]

SUMMARY

Sodium glucose cotransporters (SGLTs) are transport proteins that are expressed throughout the body. Inhibition of SGLTs is a relatively novel therapeutic strategy to improve glycemic control and has been shown to promote cardiorenal benefits. Dual SGLT1/2 inhibitors (SGLT1/2i) such as sotagliflozin target both SGLT1 and 2 proteins. Sotagliflozin or vehicle was administered to diabetic Akimba mice for 8 weeks at a dose of 25 mg/kg/day. Urine glucose levels, water consumption, and body weight were measured weekly. Serum, kidney, pancreas, and brain tissue were harvested under terminal anesthesia. Tissues were assessed using immunohistochemistry or ELISA techniques. Treatment with sotagliflozin promoted multiple metabolic benefits in diabetic Akimba mice resulting in decreased blood glucose and improved polydipsia. Sotagliflozin also prevented mortalities associated with diabetes. Our data suggests that there is the possibility that combined SGLT1/2i may be superior to SGLT2i in controlling glucose homeostasis and provides protection of multiple organs affected by diabetes.

INTRODUCTION

Diabetes mellitus is a chronic metabolic disease characterized by hyperglycemia. In 2021, approximately 536.6 million adults aged 20–79 years were living with diabetes. The total number of people living with diabetes is projected to rise to 643 million by 2030 and 783.2 million by 2045.[1] The impact of diabetes mellitus on quality of life is amplified by macrovascular and particularly microvascular complications associated with the disease. The associated complications of diabetes are usually treated by a combination of lifestyle modifications and pharmacotherapy. Despite the availability of a large variety of oral anti-diabetic agents, maintaining good glycemic control is often not achieved with currently used conventional therapies and significant side-effects are common. Consequently, development of anti-hyperglycemic agents with different mechanisms of action is ongoing.[2]

Sodium-glucose cotransporters (SGLTs) are transport proteins expressed on the luminal side of the cell membrane across various organs in the body. Among the family of SGLTs, SGLT1 and SGLT2 have been commonly investigated. SGLT1 is the primary transporter for glucose absorption in the gut. Its inhibition blunts and delays postprandial glucose excursion. SGLT2, located in the early renal proximal tubule, is responsible for the reabsorption of ∼90% of glucose filtered by the kidney, whereas SGLT1, located in the late proximal tubule, removes any remaining glucose.[2,3] Over the past few years, the identification of the role of SGLTs in glucose regulation and their inhibition with selective SGLT2 inhibitors (SGLT2i's) has revolutionized the treatment of diabetes. Although the primary interest in SGLT2 inhibition (SGLT2i) was related to their direct benefit in reducing hyperglycemia, they have now shown to exert unprecedented cardiorenal protective effects not only in individuals with diabetes, but also in non-diabetic patients, although the exact mechanism remains unclear.[4] Lately we and others have described pleiotropic effects of SGLT2i's such as sympathoinhibition in a wide range of target tissues throughout the body.[5–10]

Another promising therapeutic target within the SGLT family is SGLT1. SGLT1 is widely expressed in organs such as kidneys, heart, intestine, liver, pancreas, brain and eyes.[11] More recently, genetic and pharmacology research in mice has indicated that gastrointestinal SGLT1 inhibition may also be an appropriate therapeutic target to treat diabetes.[3] Combining SGLT1/2 inhibition (SGLT1/2i) in a single molecule could provide complementary insulin-independent effects to improve diabetes control and ameliorate diabetes associated complications. Indeed, the first dual SGLT1/2 inhibitor sotagliflozin (SOTAG) was developed

[1]Dobney Hypertension Centre, School of Biomedical Sciences – Royal Perth Hospital Unit / Royal Perth Hospital Medical Research Foundation, University of Western Australia, Crawley, WA 6009, Australia

[2]Research Centre, Royal Perth Hospital, Perth, WA 6000, Australia

[3]Department of Molecular Ophthalmology, University of Western Australia, Crawley, WA 6009, Australia

[4]Dobney Hypertension Centre, Medical School – Royal Perth Hospital Unit / Royal Perth Hospital Medical Research Foundation, University of Western Australia, Crawley, WA 6009, Australia

[5]Department of Cardiology and Department of Nephrology, Royal Perth Hospital, Perth, WA 6000, Australia

[6]These authors contributed equally

[7]Senior author

[8]Lead contact

*Correspondence: vance.matthews@uwa.edu.au

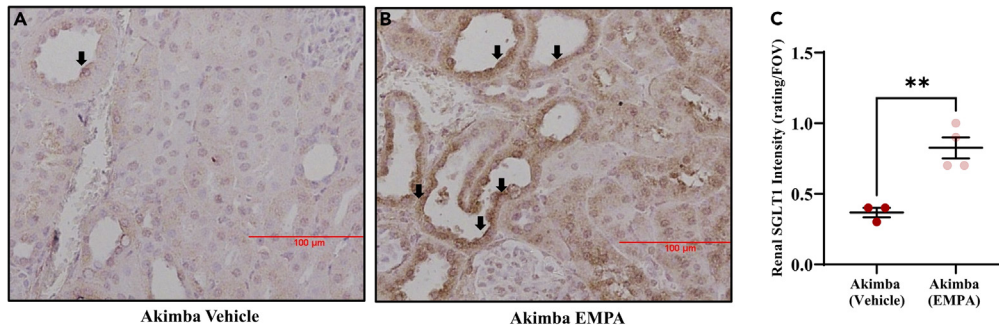https://doi.org/10.1016/j.isci.2023.107260

Figure 1. SGLT2 inhibition results in increased luminal SGLT1 expression in renal tissue of diabetic Akimba mice
(A and B) Representative SGLT1 immunohistochemistry images of renal tissue of mice treated with (A) vehicle or (B) Empagliflozin [EMPA] via drinking water (25 mg/kg/day) for 8 weeks.
(C) Quantitation of SGLT1 intensity; n = 3–4 mice/group; mean ± SEM. Statistical analysis was conducted by two-tailed Student's *t* test; **p = 0.005. Black arrow = luminal SGLT1 expression. Scale bar = 100 μm. Intensity: 0 = absent - 3 = high intensity; FOV, Field of view. See also Figures S1–S3.

and is now undergoing phase III clinical trials.[12,13] The differentiating clinical features of dual SGLT1/2i include a large postprandial glucose reduction, elevation of glucagon-like peptide 1 and modest urinary glucose excretion.[14] In addition, SGLT1/2i with SOTAG was associated with lower rates of death from cardiovascular causes, and hospitalizations and heart failure admissions compared to placebo in settings of both patients with (1) type 2 diabetes (T2D) and recent worsening heart failure (SOLOIST-WHF trial) and (2) T2D and chronic kidney disease (SCORED trial).[12,13] In type 1 diabetes (T1D), phase III clinical trials (in-Tandem1, inTandem2 and inTandem3) have shown that SOTAG reduces Hb_{A1C} levels, with secondary benefits of decreasing insulin utilization, lowers risk of severe hypoglycemia and decreased fasting glucose levels.[15]

Rieg et al., (2014) demonstrated that genetic and pharmacological inhibition of SGLT2 leads to an increase in SGLT1-mediated glucose reabsorption in the kidney in euglycemic conditions. This increase in SGLT1 activity can compensate for the reduction in glucose reabsorption caused by SGLT2 inhibition, resulting in a maintenance of glucose homeostasis.[16] We have reproducibly shown that, in diabetic Akimba mice, SGLT2i with DAPA or EMPA promotes upregulation of SGLT1 in the retina[17] or kidney as shown in our current study. These results highlight the critical requirement for dual SGLT1/2i related studies to fully understand the benefits and the mechanism of action of this drug class. Therefore, we performed investigations utilizing our well-established T1D Akimba mouse model which is a cross between the Kimba mouse model (trVEGF029) and the naturally occurring diabetic Akita (Ins2Akita) mouse model,[18] to determine the effects of dual SGLT1/2i on relevant target organs in T1D.

RESULTS

Compensatory upregulation of SGLT1 protein expression with pharmacological inhibition of SGLT2

In diabetic Akimba mice, the treatment with the specific SGLT2 inhibitor EMPA at a concentration of 25 mg/kg/day upregulated the SGLT1 protein expression in the kidney, when compared to vehicle treated Akimba mice (Figure 1). This result highlights the potential benefit of dual SGLT1 and 2 inhibition in the context of T1D. It should be noted that when the primary antibody (anti-SGLT1 antibody) is omitted, there was no brown staining observed (Figure S1). As evidence of heterogeneity in SGLT1 protein expression after SGLT2 inhibition, grading of SGLT1 expression was conducted. A majority of SGLT1 positive tubules were expressing SGLT1 at a low level (graded as 1) and SGLT2 inhibition produced a greater number of these tubules (Figure S2). We also examined *Sglt1* mRNA levels in the same kidneys as utilized in Figure 1. Upon conducting mRNA analysis for *Sglt1*, there was an absence of *Sglt1* mRNA differences between the vehicle and EMPA groups (Figure S3).

SGLT1/2 inhibition with SOTAG promoted glucosuria in non-diabetic Kimba mice

The Kimba mouse model lacks the hyperglycemic background and hence acts as an internal control to determine the effectiveness of the SGLT1/2 inhibitor SOTAG used in our study. Before treatment, urine
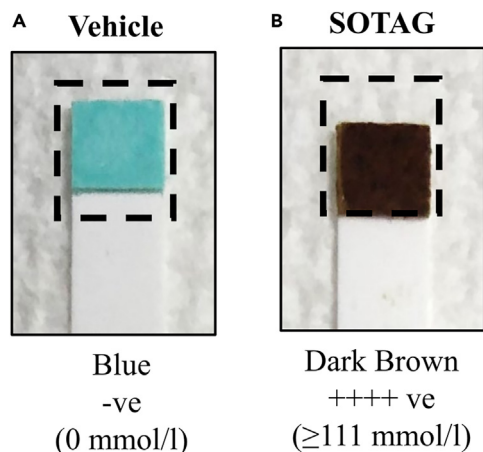
Figure 2. SOTAG promotes glucosuria in non-diabetic Kimba mice

(A and B) Representative image of glucose levels in urine in (A) Kimba mice treated with vehicle or (B) SOTAG (25 mg/kg/day); Blue = 0 mmol/L glucose, Dark brown ≥111 mmol/L glucose. SOTAG, sotagliflozin.

glucose levels in non-diabetic Kimba mice showed 0 mmol/L compared to ≥111 mmol/L in diabetic Akimba mice (data not shown). As anticipated, the consumption of SOTAG at a concentration of 25 mg/kg/day in drinking water, resulted in glucosuria in non-diabetic Kimba mice (Figure 2B) indicated by the dark brown color (≥111 mmol/L). Mice receiving vehicle remained at 0 mmol/L indicated by the blue color (Figure 2A). Irrespective of treatment, urine glucose levels of the diabetic Akimba mice were ≥111 mmol/L. In addition, all Kimba and Akimba mice showed smooth and healthy body coats, normal responses to touch, normal posture and bright eyes throughout the 8 weeks of SOTAG treatment.

Mortality rates in Akimba mice

In vehicle treated Akimba mice a 14.3% mortality rate (two out of 14 mice) was noted, whereas a 100% survival rate was observed in Akimba mice treated with SOTAG. Regardless of treatment, a 100% survival rate was observed in Kimba mice.

SOTAG treatment prevented the failure to thrive in diabetic Akimba mice

In the initial 5 weeks of treatment, Kimba mice gained weight at similar rates irrespective of treatment (Figure 3A). Typically, diabetic Akimba mice show poor weight gain, a hallmark feature of the failure to thrive phenotype in these animals. From the point of treatment commencement, Akimba mice treated with SOTAG exhibited healthy weight gain and this was significantly increased by week 5 when compared to their counterparts receiving vehicle (Figure 3B).

Treatment with SOTAG significantly reduced fasting blood glucose levels in non-diabetic Kimba and diabetic Akimba mice

Following 8 weeks of treatment with SOTAG, fasting blood glucose levels were significantly lower in non-diabetic Kimba mice (Figure 4A; 12.2 ± 1.0 mmol/L) when compared to mice receiving vehicle (Figure 4A; 15.0 ± 0.4 mmol/L). As expected, the fasting blood glucose levels in diabetic Akimba mice after 8 weeks of SOTAG treatment (Figure 4B; 18.0 ± 1.2 mmol/L) were significantly lower than vehicle treated mice (Figure 4B; 33.0 ± 0.1 mmol/L).

In addition, pancreatic tissue was examined using H&E staining. Diabetic Akimba mice showed increased islet mass after SOTAG treatment (Figures S4D and S4F) when compared to vehicle treated counterparts (Figures S4A–S4C), suggesting an improvement in pancreatic health. A histologic assessment of general islet structure indicated that pancreatic islet mass was affected by the progression of diabetes in Akimba mice, as demonstrated by the appearance of small and irregular islet architecture (Figures S4A–S4C).

SOTAG and EMPA promotes glucose tolerance in diabetic Akimba mice

As we have previously shown that SOTAG significantly lowered fasting blood glucose levels in Akimba mice, we then asked the question whether dual SGLT1/2i is more efficient at promoting glucose tolerance than SGLT2i alone with EMPA. When conducting a 120 min GTT in our vehicle, EMPA or SOTAG treated Akimba mice, it was highly evident that the vehicle treated mice were the most glucose intolerant as their
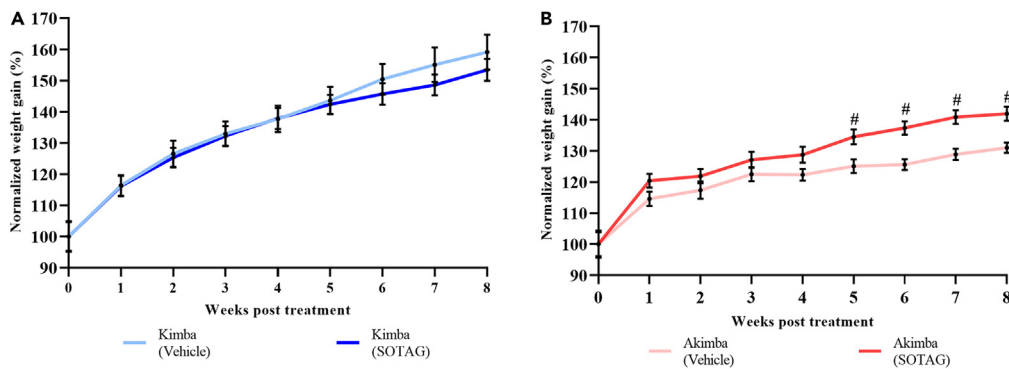
Figure 3. Effect of SOTAG on the body weight of non-diabetic Kimba and diabetic Akimba mice
(A and B) The normalized body weight percentage during 8 weeks of treatment with vehicle or SOTAG in (A) Kimba and (B) Akimba mice. Statistical analysis was conducted by two-tailed Student's t test; #$p \leq 0.01$; data represented as mean $\pm$ SEM of 12–15 mice per group. SOTAG, sotagliflozin.

fasting blood glucose started at 26.5 mmol/L at the time-point 0 min and remained the highest throughout the time-course. Alternatively, the fasting blood glucose levels in EMPA or SOTAG treated Akimba mice were markedly lower at 14.63 mmol/L and 13.6 mmol/L at time-point 0 min, respectively. There was no statistical difference in fasting blood glucose levels at time-point 0 min in Akimba mice treated with EMPA (14.6 ± 1.5 mmol/L) or SOTAG (13.6 ± 1.7 mmol/L). After glucose administration, the EMPA or SOTAG treated Akimba mice were consistently displaying lower glucose levels from 30 min onwards compared to the Akimba vehicle mice. There was no statistically discernible difference between EMPA or SOTAG treated Akimba mice (Figure 5). However, at the 45 min time-point, there was a switch whereby SOTAG treated Akimba mice had a tendency to display mildly improved glucose tolerance compared to Akimba EMPA. We also show that the non-diabetic EMPA or SOTAG treated Kimba counterparts were the most glucose tolerant mice as evidenced by their markedly lower fasting blood glucose levels over the 120 min time-course (Figure 5). As demonstrated by Area Under the Curve (AUC) analysis (Figure S5), there was no statistical difference between Akimba EMPA and SOTAG treated mice. However, the treatment of Akimba mice with either EMPA or SOTAG produced marked lowering of the AUC compared to Akimba mice treated with vehicle.

SOTAG mediated effect on glucagon protein expression in diabetic Akimba and non-diabetic Kimba mice

We next sought to determine whether SOTAG influences glucagon protein expression in pancreatic islets. When compared to vehicle treated mice, Akimba mice treated with SOTAG showed a significant increase in glucagon protein expression in pancreatic islets (Figure 6). However, in non-diabetic Kimba mice, SOTAG treatment only promoted a trend for an increase in glucagon levels (Figure S6).
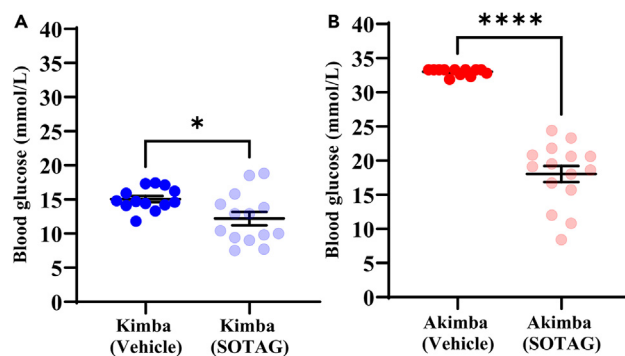

Figure 4. Administration of SOTAG on blood glucose in non-diabetic Kimba and diabetic Akimba mice
(A and B) Graphs show fasting blood glucose levels after 8 weeks of vehicle or SOTAG treatment in (A) Kimba and (B) Akimba mice. Statistical analysis was conducted by two-tailed Student's t test; *$p \leq 0.01$, ****$p \leq 0.0001$; data represented as mean $\pm$ SEM of 12–15 mice per group. SOTAG, sotagliflozin. See also Figures S4.
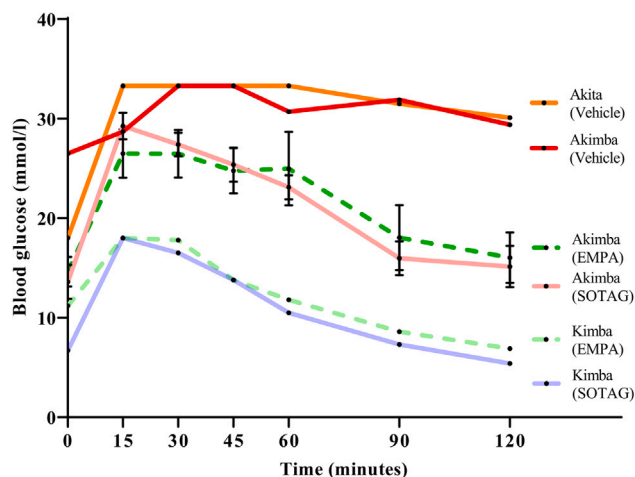
Figure 5. The effects of EMPA and SOTAG on glucose tolerance

Fasting Blood glucose levels in vehicle, EMPA or SOTAG-treated Akimba and Kimba (25 mg/kg/day for 3 weeks) mice during an intraperitoneal glucose tolerance test. For Akimba EMPA and SOTAG, n = 3 mice/group; mean ± SEM. The Akita (vehicle), Akimba (vehicle) and Kimba (EMPA and SOTAG) are individual reference mice for the purpose of representing glucose intolerant and glucose tolerant counterparts, respectively. SOTAG, sotagliflozin; EMPA, Empagliflozin; GTT, Glucose Tolerance Testing. See also Figures S5.

Treatment with SOTAG improved diabetes-associated polydipsia in Akimba mice

When compared to vehicle treated mice, SOTAG treated Kimba mice showed an increase in water intake from day 3 onwards. This increase in water intake was significant from day 10 onwards and was consistently maintained until the end of the experiment (Figure 7A). Akimba mice on both vehicle and SOTAG showed a similar water intake at day 3 and 10. However, by day 17, when compared to vehicle treated mice, SOTAG treated diabetic animals showed a reduction in water intake and this reduction was significant at day 31 onwards. By the end of the experiment, the reduction in water intake was significantly greater in SOTAG treated diabetic mice indicating improved diabetes-associated polydipsia in these animals (Figure 7B).

Effect of SOTAG on daily food intake

With respect to the diabetic Akimba mice, there was no evident effect of EMPA or SOTAG treatment on food intake compared to vehicle treatment (Figure 8A). As indicated in Figure 8B, SOTAG promoted a trend for reduced food intake compared to EMPA (p=0.057).

Treatment with SOTAG improved renal hypertrophy in diabetic Akimba mice

In order to determine whether SOTAG promotes benefits on kidney health in diabetic Akimba mice, the average Kidney to Body Weight (KW/BW) ratio was assessed after 8 weeks of therapy. In diabetic Akimba
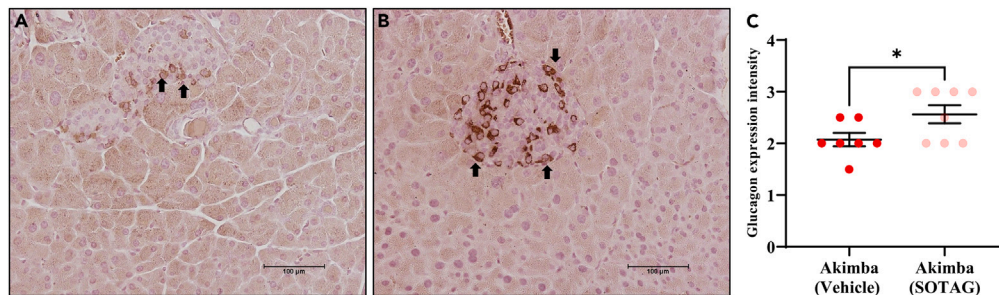

Figure 6. Effect of SOTAG on glucagon protein expression in the pancreas of diabetic Akimba mice

Representative glucagon immunohistochemistry images of pancreatic tissue of Akimba mice treated with (A) vehicle or (B) SOTAG via drinking water (25 mg/kg/day) for 8 weeks (C) Quantitation of glucagon intensity. Statistical analysis was conducted by two-tailed Student's *t* test; *p ≤ 0.05; data represented as mean ± SEM of 7–8 mice per group. Black arrow = glucagon expression. Scale bar = 100 μm. SOTAG, sotagliflozin. See also Figures S6.
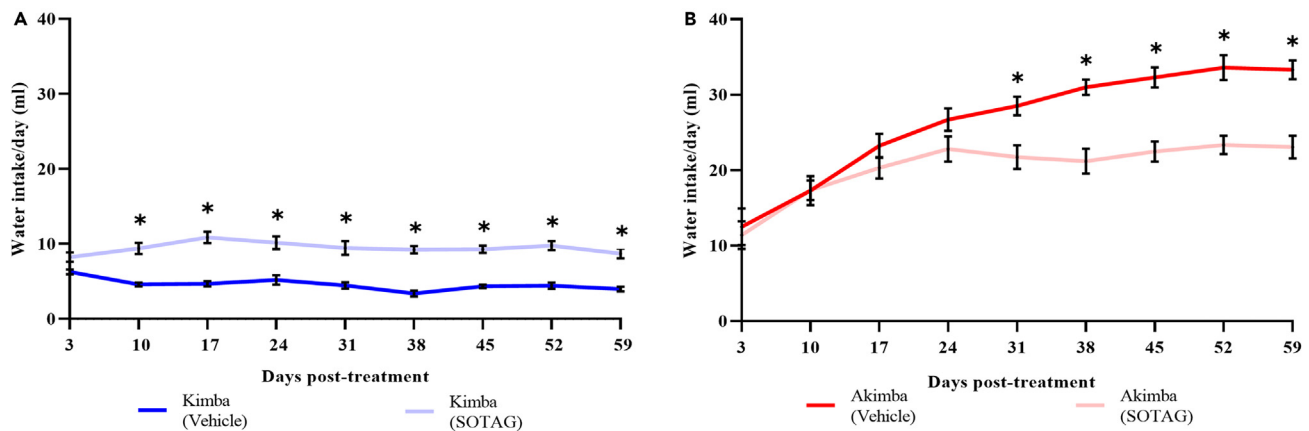
Figure 7. Effect of SOTAG on water intake in non-diabetic Kimba and diabetic Akimba mice
(A and B) Graphs show water intake in (A) Kimba and (B) Akimba mice starting from day 3 and measured every 7 days for a period of 8 weeks. Statistical analysis was conducted by two-tailed Student's *t* test; *p ≤ 0.05; data represented as mean ± SEM of 12–15 mice per group. SOTAG, sotagliflozin.

mice, SOTAG treatment significantly decreased the KW/BW ratio compared to vehicle treated counterparts (Figure 9) indicative of regression of renal hypertrophy associated with diabetes.

Dual inhibition with SOTAG promotes compensation of SGLT1 and SGLT2 in the kidneys of diabetic Akimba mice

The luminal staining intensity of SGLT1 or SGLT2 was assessed in diabetic Akimba kidneys. When compared to mice treated with vehicle, SOTAG resulted in significant upregulation of both SGLT1 (Figure 10) and SGLT2 (Figure 11) protein expression. We also examined *Sglt1* mRNA levels in the same kidneys as utilized in Figure 10. Upon conducting mRNA analysis for *Sglt1*, there was an absence of *Sglt1* mRNA differences between the vehicle and SOTAG groups (Figure S7). To demonstrate the heterogeneity in SGLT1 and SGLT2 protein expression in individual tubules following SGLT1/2 inhibition with SOTAG, we performed a grading assessment of tubular SGLT1 and SGLT2 expression. Firstly, when we conducted a detailed SGLT1 expression study for individual tubules in diabetic Akimba mice treated with vehicle or SOTAG, the majority of the tubules positive for SGLT1 exhibited low levels of expression (graded as 1) and SGLT1/2 inhibition with SOTAG resulted in an increased number of these tubules in particular (Figure S8). Furthermore, the detailed SGLT2 expression analysis of individual tubules in diabetic Akimba mice treated with vehicle or SOTAG demonstrated an extremely interesting phenomenon whereby the highest SGLT2 expression level (graded 3) occurs in the Akimba SOTAG group compared to vehicle treated mice (Figure S9A). Alternatively, the tubules graded with a low or intermediate SGLT2 expression level (graded 1 and 2, respectively) is highest in the Akimba vehicle group compared to SOTAG treatment. However, when an overall mean SGLT2 tubular intensity was
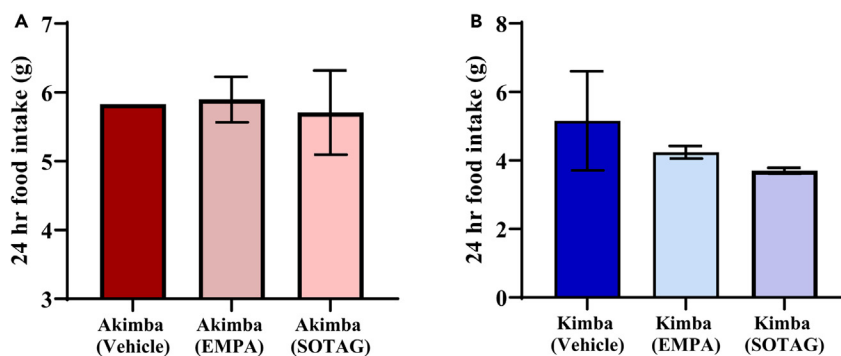

Figure 8. Food intake in diabetic Akimba and non-diabetic Kimba mice treated with EMPA or SOTAG
For Akimba (A) and Kimba (B) EMPA and SOTAG, n = 3 mice/group; mean ± SEM. The Akimba vehicle and Kimba vehicle groups have n = 1 and 2 mice, respectively for the purpose of representing diabetic and non-diabetic counterparts. SOTAG, sotagliflozin; EMPA, Empagliflozin.
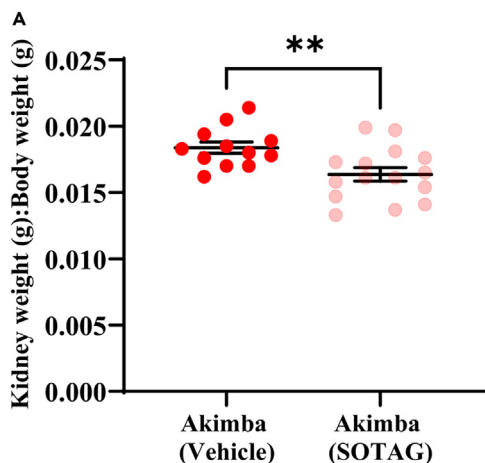
Figure 9. Treatment with SOTAG decreases the kidney to body weight ratio (KW/BW) in diabetic Akimba mice

Data represented as mean $\pm$ SEM, n = 12–15 mice/group. Statistical analysis was conducted by two-tailed Student's t test; **p $\leq$ 0.01 (Akimba vehicle vs. SOTAG). SOTAG, sotagliflozin.

measured from our detailed study, the Akimba (SOTAG) group has an overall elevated SGLT2 tubular intensity compared to the vehicle group (Figure S9B) and this supports our data already presented in Figure 11.

Treatment with SOTAG reduces activation of the sympathetic nervous system (SNS) in type 1 diabetic Akimba mice

Over-activation of the SNS is strongly associated with diabetes, disorders of the heart and kidneys (cardiorenal syndrome), obesity and hypertension.[5,7] In particular, the sympathetic overdrive in cardiovascular disease is known to trigger a number of adverse effects that are both structural and functional in nature. To determine whether treatment with SOTAG may decrease SNS activity, we examined Norepinephrine (NE) levels in kidney lysates. For the first time, we have shown that NE, the major neurotransmitter of the SNS is significantly decreased in SOTAG treated diabetic Akimba mice when compared to vehicle treated controls (Figure 12).

Effect of SOTAG on diabetes-related proinflammatory cytokines

A large number of studies suggest that inflammatory mechanisms play a critical role in the pathogenesis of diabetes mellitus.[19] Therefore, we assessed the diabetes-associated proinflammatory cytokines TNF-α and IL-6 in the kidneys of diabetic Akimba mice treated with vehicle or SOTAG. Of interest, treatment with SOTAG decreased the pro-inflammatory cytokine IL-6 and did not alter TNF-α levels (Figure 13) when compared to vehicle treated mice.

Effect of SOTAG on the diabetes brain tyrosine hydroxylase (TH) levels

Evidence suggests that reduced TH-immunoreactivity in the substantia nigra of diabetic animals may potentially lead to motor abnormalities.[20] Decreased TH-immunoreactivity in the brain has also been

Figure 10. SOTAG promotes over expression of SGLT1 protein levels in the kidneys of diabetic Akimba mice

(A and B) Representative SGLT1 immunohistochemistry images of renal tissue of mice treated with (A) vehicle or (B) SOTAG via drinking water (25 mg/kg/day) for 8 weeks.

(C) Quantitation of SGLT1 intensity. Statistical analysis was conducted by two-tailed Student's t test; *p $\leq$ 0.05; data represented as mean $\pm$ SEM of 5 mice per group. Black arrow = luminal SGLT1 expression. Scale bar = 100 μm. SGLT1, Sodium glucose cotransporter 1; SOTAG, sotagliflozin. See also Figures S1, S7, and S8.
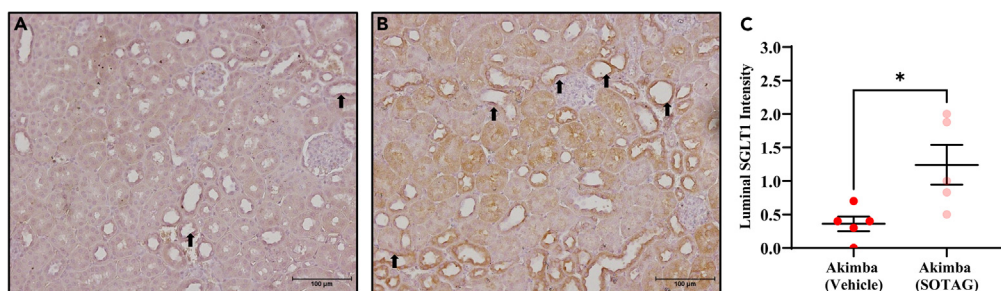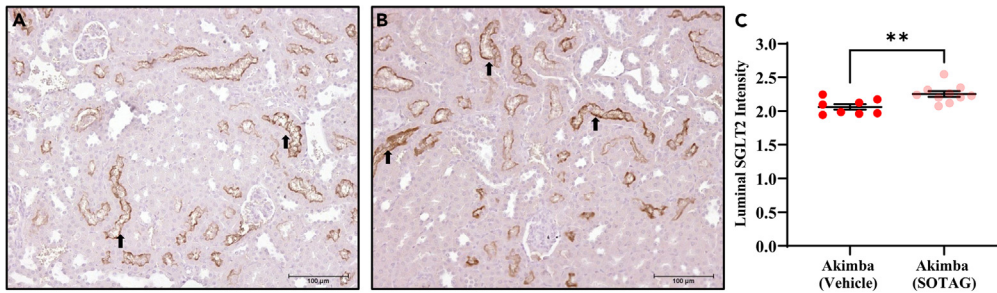
Figure 11. SOTAG promotes over expression of SGLT2 protein levels in the kidneys of diabetic Akimba mice

(A and B) Representative SGLT2 immunohistochemistry images of renal tissue of mice treated with (A) vehicle or (B) SOTAG via drinking water (25 mg/kg/day) for 8 weeks.

(C) Quantitation of SGLT2 intensity. Statistical analysis was conducted by two-tailed Student's *t* test; **p ≤ 0.01; data represented as mean ± SEM of 8–10 mice per group. Black arrow = luminal SGLT2 expression. Scale bar = 100 μm. SGLT2, Sodium glucose cotransporter 2; SOTAG, sotagliflozin. See also Figures S9.

associated with aging.[21] Furthermore, TH protein content is decreased in the surviving nigral dopaminergic neurons in Parkinson's disease.[22] Therefore, we were interested in assessing the influence of SOTAG on brain TH expression levels. Of interest, for the first-time, we provide evidence of increased TH-positivity in the SOTAG treated Akimba brain when compared to vehicle treated mice (Figure S10), perhaps pointing to additional central beneficial effects of SOTAG in the setting of T1D.

DISCUSSION

SGLTs are transport proteins that are expressed in various organs throughout the body. The two main family members of interest are SGLT1 and SGLT2. The SGLT2 protein is predominantly found in the kidneys and our team has shown that it is also expressed in the retina of the eye.[9] SGLT2 inhibitors (SGLT2i) reduce glucose and sodium reabsorption as a result of glucosuria and natriuresis. Furthermore, they have been associated with cardiorenal protection. Unlike SGLT2, which is mostly limited to expression in the kidneys and the retina, SGLT1 is more widely distributed throughout the body. Although predominantly expressed in the apical membrane of the small intestine,[23] it is also highly expressed in the cardiomyocytes of the heart,[23] the kidney, and, as recently demonstrated by us, also in the retina.[17] In studying the effects of SGLT2i in a mouse model of diabetes, we discovered that the SGLT2 inhibition results in a marked upregulation of SGLT1 expression in both the kidneys and the retina of treated animals. Another study also showed that the SGLT2i Dapagliflozin upregulates SGLT1 expression in pancreatic α-cells.[24] Taken together, this supports the notion that SGLT1 is upregulated in a multitude of organs and most importantly, SGLT2i promotes a compensatory elevation in SGLT1 expression, thereby potentially diminishing both glucose-related and organ specific benefits of SGLT2i.

Our studies have shown that when the dual SGLT1/2i sotagliflozin (SOTAG) is administered to type 1 diabetic Akimba mice, there is a further improvement in metabolic parameters and markers of renal damage compared
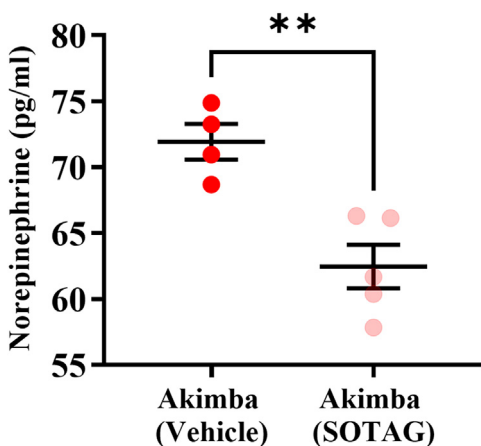

Figure 12. Sympathoinhibition is mediated by SOTAG in diabetic Akimba mice

Norepinephrine (NE) content is significantly reduced in kidney lysates of Akimba mice treated with SOTAG. n = 4–5 mice/group; mean ± SEM. Statistical analysis was conducted by two-tailed Student's *t* test; **p ≤ 0.01 vs. Vehicle. SOTAG, sotagliflozin.
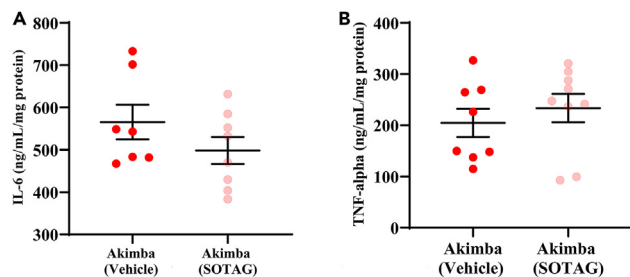
Figure 13. Effect of SOTAG on diabetes-related proinflammatory cytokines in Akimba mice
(A and B) (A) IL-6 and (B) TNF-α levels in kidney lysates of Akimba mice treated with vehicle vs. SOTAG. n = 7–9 mice/group; mean ± SEM. SOTAG, sotagliflozin.

to treatment with the SGLT2i Empagliflozin alone.[9] We have shown that SOTAG promoted an even greater level of glucosuria than Empagliflozin, resulting in an additional 4-5 mmol/L decrease in fasting blood glucose levels.[9] Additionally, SOTAG produced an improvement in the diabetic phenotype, causing a more pronounced reduction in polydipsia and failure to thrive phenotype than SGLT2i alone.

We report, for the first time, the side-by-side comparison of glucose tolerance in type 1 diabetic mice treated with EMPA or SOTAG. Similar to our findings, both EMPA[25] and SOTAG[26] have been shown to promote glucose tolerance in diabetic animals. Although not significant, we observed a mildly greater glucose tolerance in diabetic mice treated with SOTAG when compared to EMPA. It can be hypothesized that SOTAG-mediated inhibition of intestinal glucose absorption is associated with the further improvement in glucose tolerance observed in Akimba mice. However, future studies should be conducted after longer treatment durations comparing the effects of EMPA and SOTAG. In addition, it should be noted that oral glucose tolerance testing is a preferable technique as it simulates real-life glucose ingestion. Hence, future studies should aim to conduct oral glucose tolerance tests in these animals.

Osmotic diuresis is a passive diuretic mechanism resulting from abnormal urinary concentrations of osmotically active solutes such as glucose or sodium.[27] It is well known that SGLT family inhibitors increase urinary glucose and Na+ excretion with concomitant osmotic diuresis. In the absence of a compensatory increase in food and fluid intake in response to SGLT2 inhibition, the kidney enhances fluid reabsorption to maintain body fluid volume. Masuda et al., (2018) reported that in non-diabetic rats with free access to food and water, SGLT2 inhibition increased glucosuria, urine volume, and Na+ excretion, which was associated with increased fluid intake.[28] Similarly, in non-diabetic Kimba mice, the mechanism of action of SOTAG caused hyperosmolar urine (due to the presence of Na+ and glucose) leading to polyuria (excessive urination), because of osmotic diuresis. This potentially was responsible for polydipsia (excessive thirst resulting in increased fluid intake) noted in these animals. It can be suggested that the increase in fluid intake in response to SGLT1/2 inhibition assisted to compensate for the primary diuretic, glucosuric, and natriuretic effect of SOTAG to maintain fluid and electrolyte balance.[28]

We have previously shown that non-diabetic Kimba mice displayed increased body weight compared to diabetic Akimba mice. In addition, treatment with EMPA reduced the weight gain tendency in non-diabetic Kimba mice.[9,29] We observed similar effects with SOTAG treatment in non-diabetic Kimba mice. Both EMPA[30] and SOTAG have been shown to prevent weight gain in non-diabetics.[26] It can be suggested that the weight loss observed with sole SGLT2 inhibition and dual SGLT1/2 inhibition is primarily because of increased calorie loss through glucosuria, resulting in a reduction in overall calorie absorption.[31,32] However, in comparison to sole SGLT2 inhibition with EMPA, dual SGLT1/2 inhibition with SOTAG partially blocks intestinal SGLT1 and increases the secretion of GLP-1,[33] which acts on the brain to induce satiety and reduce appetite.[33–35] Thus, in this study SOTAG may have contributed to the further reduction in food intake in non-diabetic Kimba mice, when compared to EMPA. However, future long-term studies should be conducted in these mouse models with EMPA and SOTAG to determine the relationship between weight loss and food intake.

Kidney hypertrophy is considered the earliest structural change noted in T1D associated kidney disease.[36] Similar to single SGLT2 inhibition,[10] SOTAG also showed a significant reduction in the KW/BW ratio in the setting of T1D, signifying that dual SGLT1/2i may improve renal health because of reduced renal hypertrophy.

In this study, we show that EMPA treatment in Akimba mice promoted a compensatory upregulation of SGLT1 protein levels in the kidney. Additionally, we investigated the effect of SOTAG treatment on SGLT1 and SGLT2 protein expression in diabetic Akimba mouse kidneys. Our results showed a significant increase in the luminal staining intensity of both SGLT1 and SGLT2 proteins in the SOTAG-treated group when compared to the vehicle-treated group, suggesting that SOTAG treatment may lead to an increase in glucose reabsorption in the proximal tubules of the kidneys, which could influence the overall glucose-lowering effect exerted by SOTAG. However, the glucose lowering effect of EMPA and SOTAG after 3 weeks of treatment was not significantly different as observed with glucose tolerance testing (Figure 5). It can be hypothesized that a longer treatment regimen may show an overall glucose-lowering effect difference between EMPA and SOTAG.

Of interest, our examination of *Sglt1* mRNA levels in the same kidneys as our protein studies did not show any differences between the respective vehicle and EMPA or vehicle and SOTAG groups. This lack of difference in mRNA levels suggests that the observed increase in SGLT1 protein expression could likely be because of post-transcriptional modifications.[37–39] However, it is important to note that the kidney tissues in this study were collected 8 weeks after treatment, and it is possible that earlier time-points may show mRNA-level differences. Therefore, further studies where tissues are collected at earlier time-points may help elucidate the mechanism of SOTAG-mediated upregulation of SGLT1 protein expression. In addition, future studies should aim to determine the effect of EMPA and SOTAG on *Sglt1* mRNA levels in various organs, given the wide expression pattern of SGLT1 in many tissues. However, it is noteworthy to emphasize the significance of examining protein levels, which we have demonstrated in our present study, as it is functional and directly influences cellular processes.[40]

Bonner et al., (2015) have shown that SGLT2i promotes an upregulation of glucagon synthesis in the pancreas of diabetic mice.[41] Similarly, our studies are the first to demonstrate that SOTAG treatment in type 1 diabetic mice promoted a significant increase in glucagon expression. We believe that this is a mechanism to prevent hypoglycemia occurring because of the glucose lowering effect of SOTAG.

As evident by our findings and other studies, inhibiting SGLT1 indeed has a beneficial outcome in relation to improving glycemic control in diabetes.[3,6,12–15] However, inhibition of SGLT1 is also known to have negative consequences such as malabsorption.[42] It is well-established that SGLT1 is responsible for the absorption of glucose and galactose in the small intestine. Therefore, the inhibition of SGLT1 can lead to a decrease in the absorption of sugars, resulting in gastrointestinal side effects such as diarrhea, abdominal pain, and flatulence.[43] In addition, inhibition of SGLT1 may be associated with osmotic diuresis, dehydration and electrolyte imbalances.[44]

T1D is now recognized as a disease of great heterogeneity. Novel therapeutics are urgently required to not only deal with the hyperglycemia but also to prevent or halt β-cell destruction[45] and reduce the over secretion of glucagon from the α-cells. Although it has been proposed that T1D prompted a linear decline in β-cell function, it has now been shown that this decline is not actually linear and can differ between patients, with some long-standing T1D patients still possessing functional β-cells[46] and with it being known that SGLT1 is only expressed in some β-cells and not others.[6]

There are many factors which underly the differences in results between patients of the same cohort. These include (1) age of onset, (2) progression of disease, (3) islet inflammation, (4) autoantibody profile, and (5) endoplasmic reticulum (ER) stress.[47]

In our experiments, we attempted to remove variation as much as feasible by using male Akimba mice (which is the sex that promotes the most reproducible phenotype), housing mice in individual cages (to avoid aggression in mice, to measure water intake accurately and to minimize soiling of cages) and finally providing mice with the same availability to water and wet mash. However, there have been studies showcasing that although single housing reduces the corticosterone levels compared to group housing, the social isolation from single housing can result in increased non-fasted blood glucose levels and glycemic variability.[48] There is also a study showing that the single housing can lead to greater levels of nesting as well as lowered weight compared to those in group housing, indicating possible thermic stress.[49]

The Akimba mouse model begins to develop diabetes around 5 weeks of age.[18] Hence, our project aimed to use younger mice in an attempt to see if we could prevent the pathogenesis of diabetes with SOTAG

before its progression. Of interest, human studies have shown that children diagnosed with T1D before age 7 have a more rapid loss of β-cell function than those diagnosed at a later age.[50] However, we must consider the biological individuality of our mice, which means that our mice will still develop T1D at slightly different ages and rates depending on other factors including pathogenic cytokine production and ER stress because of incorrectly folded insulin.[51]

Genetic predisposition is strongly associated with T1D but there are many environmental factors which trigger ER stress, therefore contributing to T1D onset and progression. Factors such as viral infections, toxins, reactive oxygen species (ROS) and chronic inflammation are all linked to exacerbating ER stress.[52] To uncover the heterogeneity in regard to ER stress in our study, further studies are warranted to test various inflammatory cytokines and levels of nitric oxide, c-peptide and autoimmune antibodies.

Hyperactivation of the SNS may contribute to hyperglycemia that is observed in diabetes. Our previous studies have shown that SGLT2i promotes sympathoinhibition by significantly reducing tyrosine hydroxylase levels and norepinephrine levels.[5,7] In line with these earlier findings, we demonstrated that combined SGLT1/2 inhibition with SOTAG also results in reduced NE content in renal tissue lysate, highlighting once more an important regulatory role of neural signaling in diabetes.

Future studies investigating the impact of SOTAG on the microbiome in the gut are also warranted, as the literature has shown that SGLT2 inhibitors like Canagliflozin[53] and SGLT1 inhibitor SGL5213[54] increase short chain fatty acids in the gut and therefore reduces gut derived uremic toxins leading to renal protection.

During our experiments, there were two cases of mortality (14.3%), both because of possible dehydration. Because both mice were on vehicle, it highlights the possible protective effects associated with SOTAG.

In summary, our study has highlighted that compensatory upregulation of SGLT1 could mitigate the beneficial clinical effects of SGLT2i, whereas combined inhibition of SGLT1/2 may augment the clinical benefit. Our data suggests that combined SGLT1/2i may be superior to SGLT2i alone in controlling glucose homeostasis and providing renoprotection in diabetes.

Limitations of the study

To maintain hormonal stability and reduce variability, our studies were conducted using male mice. This approach allowed minimization of potential confounding factors arising from hormonal fluctuations in female mice.

Aiming to provide a uniform treatment protocol and facilitate comparative analysis between the two inhibitors Sotagliflozin and Empagliflozin, we administered an optimized dosage of 25 mg/kg/day. Therefore, future studies should investigate the dose-dependent effects of these inhibitors.

Dissection of tissues was carried out at 8 weeks after treatment. However, to facilitate the identification of the optimal tissue collection time point, detailed time course studies should be considered in future experiments.

All treatments (vehicle, Sotagliflozin, and Empagliflozin) were administered via drinking water. Future studies should explore the possibility of conducting oral gavage therapy as an alternative drug administration route.

In this study, glucose tolerance testing was performed using intraperitoneal administration of glucose. However, in future investigations, oral administration of glucose during glucose tolerance testing may offer closer resemblance to physiological conditions. In addition, blood glucose levels were determined via tail vein sampling. Future experiments using real-time continuous glucose monitoring with telemetry may offer more comprehensive assessment of glucose fluctuations and responses to treatment.

STAR★METHODS

Detailed methods are provided in the online version of this paper and include the following:

- KEY RESOURCES TABLE
- RESOURCE AVAILABILITY

- ○ Lead contact
- ○ Materials availability
- ○ Data and code availability
- ● EXPERIMENTAL MODEL AND STUDY PARTICIPANT DETAILS
  - ○ Animal models and genotyping
  - ○ Animal experiments
- ● METHOD DETAILS
  - ○ Glucose tolerance testing (GTT)
  - ○ Specimen collection
  - ○ Determination of gene expression
  - ○ H&E, tyrosine hydroxylase, glucagon, SGLT1 and SGLT2 immunohistochemistry
  - ○ Tissue section imaging and analysis
  - ○ Enzyme-linked immunosorbent assays
- ● QUANTIFICATION AND STATISTICAL ANALYSIS

SUPPLEMENTAL INFORMATION

Supplemental information can be found online at https://doi.org/10.1016/j.isci.2023.107260.

AUTHOR CONTRIBUTIONS

V.B.M., M.P.S., and L.Y.H. conceptualized the research study. L.Y.H., V.B.M., M.P.S., and E.P.R. funding acquisition. E.P.R. generated the transgenic mice. V.B.M. supervised the entire study and analyzed the data with L.Y.H. and J.R.M. L.Y.H., J.R.M., V.B.M., and M.H. performed experiments. L.Y.H. and V.B.M. generated the figures. L.Y.H., J.R.M., and V.B.M. writing – original draft. V.B.M. and M.P.S. provided useful suggestions and edited the manuscript. L.Y.H. and V.B.M. revised the manuscript.

DECLARATION OF INTERESTS

All the authors declare no competing interests.

INCLUSION AND DIVERSITY

We support inclusive, diverse, and equitable conduct of research.

REFERENCES

1. Sun, H., Saeedi, P., Karuranga, S., Pinkepank, M., Ogurtsova, K., Duncan, B.B., Stein, C., Basit, A., Chan, J.C.N., Mbanya, J.C., et al. (2022). IDF Diabetes Atlas: Global, regional and country-level diabetes prevalence estimates for 2021 and projections for 2045. Diabetes Res. Clin. Pract. *183*, 109119. https://doi.org/10.1016/j.diabres.2021.109119.

2. Gallo, L.A., Wright, E.M., and Vallon, V. (2015). Probing SGLT2 as a therapeutic target for diabetes: basic physiology and consequences. Diabetes Vasc. Dis. Res. *12*,

78–89. https://doi.org/10.1177/1479164114561992.

3. Lapuerta, P., Zambrowicz, B., Strumph, P., and Sands, A. (2015). Development of sotagliflozin, a dual sodium-dependent glucose transporter 1/2 inhibitor. Diabetes Vasc. Dis. Res. *12*, 101–110. https://doi.org/10.1177/1479164114563304.

4. Patel, D.K., and Strong, J. (2019). The Pleiotropic Effects of Sodium-Glucose Cotransporter-2 Inhibitors: Beyond the Glycemic Benefit.

Diabetes Ther. *10*, 1771–1792. https://doi.org/10.1007/s13300-019-00686-z.

5. Matthews, V.B., Elliot, R.H., Rudnicka, C., Hricova, J., Herat, L., and Schlaich, M.P. (2017). Role of the sympathetic nervous system in regulation of the sodium glucose cotransporter 2. J. Hypertens. *35*, 2059–2068. https://doi.org/10.1097/HJH.0000000000001434.

6. Suga, T., Kikuchi, O., Kobayashi, M., Matsui, S., Yokota-Hashimoto, H., Wada, E., Kohno,

D., Sasaki, T., Takeuchi, K., Kakizaki, S., et al. (2019). SGLT1 in pancreatic α cells regulates glucagon secretion in mice, possibly explaining the distinct effects of SGLT2 inhibitors on plasma glucagon levels. Mol. Metabol. *19*, 1–12. https://doi.org/10.1016/j.molmet.2018.10.009.

7. Herat, L.Y., Magno, A.L., Rudnicka, C., Hricova, J., Carnagarin, R., Ward, N.C., Arcambal, A., Kiuchi, M.G., Head, G.A., Schlaich, M.P., and Matthews, V.B. (2020). SGLT2 Inhibitor-Induced Sympathoinhibition: A Novel Mechanism for Cardiorenal Protection. JACC. Basic Transl. Sci. *5*, 169–179. https://doi.org/10.1016/j.jacbts.2019.11.007.

8. Herat, L.Y., Ward, N.C., Magno, A.L., Rakoczy, E.P., Kiuchi, M.G., Schlaich, M.P., and Matthews, V.B. (2020). Sodium glucose co-transporter 2 inhibition reduces succinate levels in diabetic mice. World J. Gastroenterol. *26*, 3225–3235. https://doi.org/10.3748/wjg.v26.i23.3225.

9. Matthews, J., Herat, L., Rooney, J., Rakoczy, E., Schlaich, M., and Matthews, V.B. (2022). Determining the role of SGLT2 inhibition with Empagliflozin in the development of diabetic retinopathy. Biosci. Rep. *42*. https://doi.org/10.1042/BSR20212209.

10. Matthews, J.R., Schlaich, M.P., Rakoczy, E.P., Matthews, V.B., and Herat, L.Y. (2022). The Effect of SGLT2 Inhibition on Diabetic Kidney Disease in a Model of Diabetic Retinopathy. Biomedicines *10*, 522. https://doi.org/10.3390/biomedicines10030522.

11. Sano, R., Shinozaki, Y., and Ohta, T. (2020). Sodium-glucose cotransporters: Functional properties and pharmaceutical potential. J. Diabetes Investig. *11*, 770–782. https://doi.org/10.1111/jdi.13255.

12. Bhatt, D.L., Szarek, M., Pitt, B., Cannon, C.P., Leiter, L.A., McGuire, D.K., Lewis, J.B., Riddle, M.C., Inzucchi, S.E., Kosiborod, M.N., et al. (2021). Sotagliflozin in Patients with Diabetes and Chronic Kidney Disease. N. Engl. J. Med. *384*, 129–139. https://doi.org/10.1056/NEJMoa2030186.

13. Bhatt, D.L., Szarek, M., Steg, P.G., Cannon, C.P., Leiter, L.A., McGuire, D.K., Lewis, J.B., Riddle, M.C., Voors, A.A., Metra, M., et al. (2021). Sotagliflozin in Patients with Diabetes and Recent Worsening Heart Failure. N. Engl. J. Med. *384*, 117–128. https://doi.org/10.1056/NEJMoa2030183.

14. Cefalo, C.M.A., Cinti, F., Moffa, S., Impronta, F., Sorice, G.P., Mezza, T., Pontecorvi, A., and Giaccari, A. (2019). Sotagliflozin, the first dual SGLT inhibitor: current outlook and perspectives. Cardiovasc. Diabetol. *18*, 20. https://doi.org/10.1186/s12933-019-0828-y.

15. Nuffer, W., Williams, B., and Trujillo, J.M. (2019). A review of sotagliflozin for use in type 1 diabetes. Ther. Adv. Endocrinol. Metab. *10*. https://doi.org/10.1177/2042018819890527.

16. Rieg, T., Masuda, T., Gerasimova, M., Mayoux, E., Platt, K., Powell, D.R., Thomson, S.C., Koepsell, H., and Vallon, V. (2014). Increase in SGLT1-mediated transport explains renal glucose reabsorption during

genetic and pharmacological SGLT2 inhibition in euglycemia. Am. J. Physiol. Ren. Physiol. *306*, F188–F193. https://doi.org/10.1152/ajprenal.00518.2013.

17. Herat, L.Y., Matthews, J.R., Ong, W.E., Rakoczy, E.P., Schlaich, M.P., and Matthews, V.B. (2022). Determining The Role of SGLT2 Inhibition with Dapagliflozin in The Development of Diabetic Retinopathy. Front. Biosci. *27*, 321. https://doi.org/10.31083/j.fbl2712321.

18. Rakoczy, E.P., Ali Rahman, I.S., Binz, N., Li, C.R., Vagaja, N.N., de Pinho, M., and Lai, C.M. (2010). Characterization of a mouse model of hyperglycemia and retinal neovascularization. Am. J. Pathol. *177*, 2659–2670. https://doi.org/10.2353/ajpath.2010.090883.

19. Tsalamandris, S., Antonopoulos, A.S., Oikonomou, E., Papamikroulis, G.A., Vogiatzi, G., Papaioannou, S., Deftereos, S., and Tousoulis, D. (2019). The Role of Inflammation in Diabetes: Current Concepts and Future Perspectives. Eur. Cardiol. *14*, 50–59. https://doi.org/10.15420/ecr.2018.33.1.

20. Nascimento, P.S.d., Lovatel, G.A., Barbosa, S., Ilha, J., Centenaro, L.A., Malysz, T., Xavier, L.L., Schaan, B.D., and Achaval, M. (2011). Treadmill training improves motor skills and increases tyrosine hydroxylase immunoreactivity in the substantia nigra pars compacta in diabetic rats. Brain Res. *1382*, 173–180. https://doi.org/10.1016/j.brainres.2011.01.063.

21. Norrara, B., Fiuza, F.P., Arrais, A.C., Costa, I.M., Santos, J.R., Engelberth, R.C.G.J., Cavalcante, J.S., Guzen, F.P., Cavalcanti, J.R.L.P., and Freire, M.A.M. (2018). Pattern of tyrosine hydroxylase expression during aging of mesolimbic pathway of the rat. J. Chem. Neuroanat. *92*, 83–91. https://doi.org/10.1016/j.jchemneu.2018.05.004.

22. Kastner, A., Hirsch, E.C., Agid, Y., and Javoy-Agid, F. (1993). Tyrosine hydroxylase protein and messenger RNA in the dopaminergic nigral neurons of patients with Parkinson's disease. Brain Res. *606*, 341–345. https://doi.org/10.1016/0006-8993(93)91005-d.

23. Zhou, L., Cryan, E.V., D'Andrea, M.R., Belkowski, S., Conway, B.R., and Demarest, K.T. (2003). Human cardiomyocytes express high level of Na+/glucose cotransporter 1 (SGLT1). J. Cell. Biochem. *90*, 339–346. https://doi.org/10.1002/jcb.10631.

24. Solini, A., Sebastiani, G., Nigi, L., Santini, E., Rossi, C., and Dotta, F. (2017). Dapagliflozin modulates glucagon secretion in an SGLT2-independent manner in murine alpha cells. Diabetes Metab. *43*, 512–520. https://doi.org/10.1016/j.diabet.2017.04.002.

25. Daems, C., Welsch, S., Boughaleb, H., Vanderroost, J., Robert, A., Sokal, E., and Lysy, P.A. (2019). Early Treatment with Empagliflozin and GABA Improves beta-Cell Mass and Glucose Tolerance in Streptozotocin-Treated Mice. J. Diabetes Res. *2019*, 2813489. https://doi.org/10.1155/2019/2813489.

26. Powell, D.R., DaCosta, C.M., Smith, M., Doree, D., Harris, A., Buhring, L., Heydorn, W., Nouraldeen, A., Xiong, W., Yalamanchili, P., et al. (2014). Effect of LX4211 on glucose homeostasis and body composition in preclinical models. J. Pharmacol. Exp. Therapeut. *350*, 232–242. https://doi.org/10.1124/jpet.114.214304.

27. Francey, T. (2015). Chapter 160 - Diuretics. In Small Animal Critical Care Medicine, Second Edition, D.C. Silverstein and K. Hopper, eds. (W.B. Saunders), pp. 846–850. https://doi.org/10.1016/B978-1-4557-0306-7.00160-4.

28. Masuda, T., Watanabe, Y., Fukuda, K., Watanabe, M., Onishi, A., Ohara, K., Imai, T., Koepsell, H., Muto, S., Vallon, V., and Nagata, D. (2018). Unmasking a sustained negative effect of SGLT2 inhibition on body fluid volume in the rat. Am. J. Physiol. Ren. Physiol. *315*, F653–F664. https://doi.org/10.1152/ajprenal.00143.

29. Herat, L.Y., Matthews, J.R., Rakoczy, E.P., Schlaich, M.P., and Matthews, V.B. (2023). Comparing and contrasting the effects of the SGLT inhibitors Canagliflozin and Empagliflozin on the progression of retinopathy. Front. Biosci. *28*, 83. https://doi.org/10.31083/j.fbl2804083.

30. Vallon, V., Gerasimova, M., Rose, M.A., Masuda, T., Satriano, J., Mayoux, E., Koepsell, H., Thomson, S.C., and Rieg, T. (2014). SGLT2 inhibitor empagliflozin reduces renal growth and albuminuria in proportion to hyperglycemia and prevents glomerular hyperfiltration in diabetic Akita mice. Am. J. Physiol. Ren. Physiol. *306*, F194–F204. https://doi.org/10.1152/ajprenal.00520.2013.

31. Lee, P.C., Ganguly, S., and Goh, S.Y. (2018). Weight loss associated with sodium-glucose cotransporter-2 inhibition: a review of evidence and underlying mechanisms. Obes. Rev. *19*, 1630–1641. https://doi.org/10.1111/obr.12755.

32. He, Y.L., Haynes, W., Meyers, C.D., Amer, A., Zhang, Y., Mahling, P., Mendonza, A.E., Ma, S., Chutkow, W., and Bachman, E. (2019). The effects of licogliflozin, a dual SGLT1/2 inhibitor, on body weight in obese patients with or without diabetes. Diabetes Obes. Metabol. *21*, 1311–1321. https://doi.org/10.1111/dom.13654.

33. Haider, K., Pathak, A., Rohilla, A., Haider, M.R., Ahmad, K., and Yar, M.S. (2019). Synthetic strategy and SAR studies of C-glucoside heteroaryls as SGLT2 inhibitor: A review. Eur. J. Med. Chem. *184*, 111773. https://doi.org/10.1016/j.ejmech.2019.111773.

34. Krieger, J.-P. (2020). Intestinal glucagon-like peptide-1 effects on food intake: Physiological relevance and emerging mechanisms. Peptides *131*, 170342. https://doi.org/10.1016/j.peptides.2020.170342.

35. Shah, M., and Vella, A. (2014). Effects of GLP-1 on appetite and weight. Rev. Endocr. Metab. Disord. *15*, 181–187. https://doi.org/10.1007/s11154-014-9289-5.

36. Lambers Heerspink, H.J., Fioretto, P., and de Zeeuw, D. (2014). 25 - Pathogenesis,

Pathophysiology, and Treatment of Diabetic Nephropathy. In National Kidney Foundation Primer on Kidney Diseases, Sixth Edition, S.J. Gilbert and D.E. Weiner, eds. (W.B. Saunders), pp. 222–234. https://doi.org/10.1016/B978-1-4557-4617-0.00025-X.

37. Liu, Y., Beyer, A., and Aebersold, R. (2016). On the Dependency of Cellular Protein Levels on mRNA Abundance. Cell 165, 535–550. https://doi.org/10.1016/j.cell.2016.03.014.

38. Rosca, M.G., Mustata, T.G., Kinter, M.T., Ozdemir, A.M., Kern, T.S., Szweda, L.I., Brownlee, M., Monnier, V.M., and Weiss, M.F. (2005). Glycation of mitochondrial proteins from diabetic rat kidney is associated with excess superoxide formation. Am. J. Physiol. Ren. Physiol. 289, F420–F430. https://doi.org/10.1152/ajprenal.00415.2004.

39. Wu, Q., Medina, S.G., Kushawah, G., DeVore, M.L., Castellano, L.A., Hand, J.M., Wright, M., and Bazzini, A.A. (2019). Translation affects mRNA stability in a codon-dependent manner in human cells. Elife 8, e45396. https://doi.org/10.7554/eLife.45396.

40. Cenik, C., Cenik, E.S., Byeon, G.W., Grubert, F., Candille, S.I., Spacek, D., Alsallakh, B., Tilgner, H., Araya, C.L., Tang, H., et al. (2015). Integrative analysis of RNA, translation, and protein levels reveals distinct regulatory variation across humans. Genome Res. 25, 1610–1621. https://doi.org/10.1101/gr.193342.115.

41. Bonner, C., Kerr-Conte, J., Gmyr, V., Queniat, G., Moerman, E., Thévenet, J., Beaucamps, C., Delalleau, N., Popescu, I., Malaisse, W.J., et al. (2015). Inhibition of the glucose transporter SGLT2 with dapagliflozin in pancreatic alpha cells triggers glucagon secretion. Nat. Med. 21, 512–517. https://doi.org/10.1038/nm.3828.

42. Lam, J.T., Martín, M.G., Turk, E., Hirayama, B.A., Bosshard, N.U., Steinmann, B., and Wright, E.M. (1999). Missense mutations in SGLT1 cause glucose-galactose malabsorption by trafficking defects. Biochim. Biophys. Acta 1453, 297–303. https://doi.org/10.1016/s0925-4439(98)00109-4.

43. Koepsell, H. (2020). Glucose transporters in the small intestine in health and disease. Pflügers Archiv 472, 1207–1248. https://doi.org/10.1007/s00424-020-02439-5.

44. Tsimihodimos, V., Filippas-Ntekouan, S., and Elisaf, M. (2018). SGLT1 inhibition: Pros and cons. Eur. J. Pharmacol. 838, 153–156. https://doi.org/10.1016/j.ejphar.2018.09.019.

45. Greenbaum, C.J., Beam, C.A., Boulware, D., Gitelman, S.E., Gottlieb, P.A., Herold, K.C., Lachin, J.M., McGee, P., Palmer, J.P., Pescovitz, M.D., et al. (2012). Fall in C-peptide during first 2 years from diagnosis: evidence of at least two distinct phases from composite Type 1 Diabetes TrialNet data. Diabetes 61, 2066–2073. https://doi.org/10.2337/db11-1538.

46. Keenan, H.A., Sun, J.K., Levine, J., Doria, A., Aiello, L.P., Eisenbarth, G., Bonner-Weir, S., and King, G.L. (2010). Residual insulin production and pancreatic ss-cell turnover after 50 years of diabetes: Joslin Medalist Study. Diabetes 59, 2846–2853. https://doi.org/10.2337/db10-0676.

47. Eizirik, D.L., Cardozo, A.K., and Cnop, M. (2008). The role for endoplasmic reticulum stress in diabetes mellitus. Endocr. Rev. 29, 42–61. https://doi.org/10.1210/er.2007-0015.

48. Kamakura, R., Kovalainen, M., Leppäluoto, J., Herzig, K.H., and Mäkelä, K.A. (2016). The effects of group and single housing and automated animal monitoring on urinary corticosterone levels in male C57BL/6 mice. Phys. Rep. 4, e12703. https://doi.org/10.14814/phy2.12703.

49. Jirkof, P., Bratcher, N., Medina, L., Strasburg, D., Ebert, P., and Gaskill, B.N. (2020). The effect of group size, age and handling frequency on inter-male aggression in CD 1 mice. Sci. Rep. 10, 2253. https://doi.org/10.1038/s41598-020-59012-4.

50. Ziegler, A.G., Rewers, M., Simell, O., Simell, T., Lempainen, J., Steck, A., Winkler, C., Ilonen, J., Veijola, R., Knip, M., et al. (2013). Seroconversion to multiple islet autoantibodies and risk of progression to diabetes in children. JAMA 309, 2473–2479. https://doi.org/10.1001/jama.2013.6285.

51. Engin, F. (2016). ER stress and development of type 1 diabetes. J. Invest. Med. 64, 2–6. https://doi.org/10.1097/JIM.0000000000000229.

52. Lee, H., Lee, Y.S., Harenda, Q., Pietrzak, S., Oktay, H.Z., Schreiber, S., Liao, Y., Sonthalia, S., Ciecko, A.E., Chen, Y.G., et al. (2020). Beta Cell Dedifferentiation Induced by IRE1alpha Deletion Prevents Type 1 Diabetes. Cell Metabol. 31, 822–836.e5. https://doi.org/10.1016/j.cmet.2020.03.002.

53. Mishima, E., Fukuda, S., Kanemitsu, Y., Saigusa, D., Mukawa, C., Asaji, K., Matsumoto, Y., Tsukamoto, H., Tachikawa, T., Tsukimi, T., et al. (2018). Canagliflozin reduces plasma uremic toxins and alters the intestinal microbiota composition in a chronic kidney disease mouse model. Am. J. Physiol. Ren. Physiol. 315, F824–F833. https://doi.org/10.1152/ajprenal.00314.2017.

54. Ho, H.J., Kikuchi, K., Oikawa, D., Watanabe, S., Kanemitsu, Y., Saigusa, D., Kujirai, R., Ikeda-Ohtsubo, W., Ichijo, M., Akiyama, Y., et al. (2021). SGLT-1-specific inhibition ameliorates renal failure and alters the gut microbial community in mice with adenine-induced renal failure. Phys. Rep. 9, e15092. https://doi.org/10.14814/phy2.15092.

55. van Eeden, P.E., Tee, L.B.G., Lukehurst, S., Lai, C.M., Rakoczy, E.P., Beazley, L.D., and Dunlop, S.A. (2006). Early vascular and neuronal changes in a VEGF transgenic mouse model of retinal neovascularization. Invest. Ophthalmol. Vis. Sci. 47, 4638–4645. https://doi.org/10.1167/iovs.06-0251.

56. Lai, C.-M., Dunlop, S.A., May, L.A., Gorbatov, M., Brankov, M., Shen, W.-Y., Binz, N., Lai, Y.K., Graham, C.E., Barry, C.J., et al. (2005). Generation of transgenic mice with mild and severe retinal neovascularisation. Br. J. Ophthalmol. 89, 911–916. https://doi.org/10.1136/bjo.2004.059089.

57. Barber, A.J., Antonetti, D.A., Kern, T.S., Reiter, C.E.N., Soans, R.S., Krady, J.K., Levison, S.W., Gardner, T.W., and Bronson, S.K. (2005). The Ins2Akita mouse as a model of early retinal complications in diabetes. Invest. Ophthalmol. Vis. Sci. 46, 2210–2218. https://doi.org/10.1167/iovs.04-1340.

58. Chaurasia, S.S., Lim, R.R., Parikh, B.H., Wey, Y.S., Tun, B.B., Wong, T.Y., Luu, C.D., Agrawal, R., Ghosh, A., Mortellaro, A., et al. (2018). The NLRP3 Inflammasome May Contribute to Pathologic Neovascularization in the Advanced Stages of Diabetic Retinopathy. Sci. Rep. 8, 2847. https://doi.org/10.1038/s41598-018-21198-z.

59. Wisniewska-Kruk, J., Klaassen, I., Vogels, I.M.C., Magno, A.L., Lai, C.M., Van Noorden, C.J.F., Schlingemann, R.O., and Rakoczy, E.P. (2014). Molecular analysis of blood-retinal barrier loss in the Akimba mouse, a model of advanced diabetic retinopathy. Exp. Eye Res. 122, 123–131. https://doi.org/10.1016/j.exer.2014.03.005.

60. Vagaja, N.N., Chinnery, H.R., Binz, N., Kezic, J.M., Rakoczy, E.P., and McMenamin, P.G. (2012). Changes in Murine Hyalocytes Are Valuable Early Indicators of Ocular Disease. Invest. Ophthalmol. Vis. Sci. 53, 1445–1451. https://doi.org/10.1167/iovs.11-8601.

61. Arow, M., Waldman, M., Yadin, D., Nudelman, V., Shainberg, A., Abraham, N.G., Freimark, D., Kornowski, R., Aravot, D., Hochhauser, E., and Arad, M. (2020). Sodium-glucose cotransporter 2 inhibitor Dapagliflozin attenuates diabetic cardiomyopathy. Cardiovasc. Diabetol. 19, 7. https://doi.org/10.1186/s12933-019-0980-4.

62. Pennig, J., Scherrer, P., Gissler, M.C., Anto-Michel, N., Hoppe, N., Füner, L., Härdtner, C., Stachon, P., Wolf, D., Hilgendorf, I., et al. (2019). Glucose lowering by SGLT2-inhibitor empagliflozin accelerates atherosclerosis regression in hyperglycemic STZ-diabetic mice. Sci. Rep. 9, 17937. https://doi.org/10.1038/s41598-019-54224-9.

63. Karlsson, D., Ahnmark, A., Sabirsh, A., Andréasson, A.C., Gennemark, P., Sandinge, A.S., Chen, L., Tyrberg, B., Lindén, D., and Sörhede Winzell, M. (2022). Inhibition of SGLT2 Preserves Function and Promotes Proliferation of Human Islets Cells In Vivo in Diabetic Mice. Biomedicines 10, 203. https://doi.org/10.3390/biomedicines10020203.

64. Oelze, M., Kröller-Schön, S., Welschof, P., Jansen, T., Hausding, M., Mikhed, Y., Stamm, P., Mader, M., Zinßius, E., Agdauletova, S., et al. (2014). The sodium-glucose co-transporter 2 inhibitor empagliflozin improves diabetes-induced vascular dysfunction in the streptozotocin diabetes rat model by interfering with oxidative stress and glucotoxicity. PLoS One

9, e112394. https://doi.org/10.1371/journal.pone.0112394.

65. Steven, S., Oelze, M., Hanf, A., Kröller-Schön, S., Kashani, F., Roohani, S., Welschof, P., Kopp, M., Gödtel-Armbrust, U., Xia, N., et al. (2017). The SGLT2 inhibitor empagliflozin improves the primary diabetic complications in ZDF rats. Redox Biol. *13*, 370–385. https://doi.org/10.1016/j.redox.2017.06.009.

66. Jowett, J.B.M., Okada, Y., Leedman, P.J., Curran, J.E., Johnson, M.P., Moses, E.K., Goring, H.H.H., Mochizuki, S., Blangero, J., Stone, L., et al. (2012). ADAM28 is elevated in humans with the metabolic syndrome and is a novel sheddase of human tumour necrosis factor-alpha. Immunol. Cell Biol. *90*, 966–973. https://doi.org/10.1038/icb.2012.44.

67. Fuhrich, D.G., Lessey, B.A., and Savaris, R.F. (2013). Comparison of HSCORE assessment of endometrial beta3 integrin subunit expression with digital HSCORE using computerized image analysis (ImageJ). Anal. Quant. Cytopathol. Histpathol. *35*, 210–216.

STAR★METHODS

KEY RESOURCES TABLE

REAGENT or RESOURCE	SOURCE	IDENTIFIER
Antibodies		
Mouse anti-glucagon antibody (K79bB10)	Novus Biologicals, Melbourne, Australia	NB600-1506; RRID:AB_790003
Anti-Tyrosine Hydroxylase Antibody	Merck Millipore, Sydney, Australia	AB152; RRID:AB_390204
Rabbit anti-SGLT1 Antibody	Abcam, Melbourne, Australia	ab14685; RRID:AB_301410
Rabbit anti-SGLT1 Antibody	Novus Biologicals, Melbourne, Australia	NBP220338
Rabbit anti-SGLT2 Antibody	Novus Biologicals, Littleton, CO, USA	NBP192384; RRID:AB_11027910
Mouse anti-SGLT2 Antibody	Santa Cruz Biotechnology, Santa Cruz, CA, USA	sc-393350; RRID:AB_2814658
Anti-rabbit secondary antibodies conjugated with HRP	Santa Cruz Biotechnology, Sydney, NSW, Australia	NA934V
Anti-mouse secondary antibodies conjugated with HRP	Santa Cruz Biotechnology, Sydney, NSW, Australia	NA931V
Chemicals, peptides, and recombinant proteins		
ultraView Universal DAB (3, 3′-Diaminobenzidine) detection kit	Ventana, USA	760-500
Gill's haematoxylin	Sigma-Aldrich, Sydney, Australia	GHS232-1L
DPX Mountant for histology	Sigma-Aldrich, Sydney, Australia	06522-100ML
TWEEN® 20	Sigma-Aldrich, Sydney, Australia	P1379-100ML
Ethylenediaminetetraacetic acid (EDTA)	Sigma-Aldrich, Sydney, Australia	ED-500G
Sotagliflozin	Med Chem Express, USA	Cat. No.: HY-15516
Empagliflozin	Ark Pharma Scientific Limited, Wuhan, China	H-013293
Keto-Diastix Bayer Reagent Strips	Bayer, Leverkusen, Germany	2883
Dimethylsulfoxide (DMSO)	Sigma-Aldrich, Sydney, Australia	D8418-100ML
Glucose 50% Intravenous Infusion	Phebra, Sydney, Australia	INJ128
High-Capacity RNA-to-cDNA™ Kit	Applied Biosystems, Thermo Fisher Scientific, Victoria, Australia	Cat#: 4387406
TRIzol™ Reagent	Invitrogen, Sydney, Australia	Cat#: 15596026
Taqman Gene Expression Master Mix	Applied Biosystems, Thermo Fisher Scientific, Victoria, Australia.	Catalog #: 4369016
Critical commercial assays		
Mouse Noradrenaline,NA ELISA Kit	Cusabio, Wuhan, Hubei Province, China	CSBE07870m
TNF-α ELISA Kit	elisakit.com, Melbourne, Australia	EK-0005
IL-6 ELISA Kit	elisakit.com, Melbourne, Australia	EK-0029
Experimental models: Organisms/strains		
C57BL/6-Ins2Akita/J mouse model (RRID:IMSR_JAX:003548)	Animal Resources Centre, Perth, Western Australia	N/A
Kimba mouse model (trVEGF029)	Animal Resources Centre, Perth, Western Australia	Reference 56
Akimba mouse model (Ins2AkitaVEGF+/−)	Animal Resources Centre, Perth, Western Australia	Reference 18
Oligonucleotides		
Mouse Sglt1	Applied Biosystems, Thermo Fisher Scientific, Victoria, Australia.	Mm00451203_m1

Continued

REAGENT or RESOURCE	SOURCE	IDENTIFIER
Mouse Hprt	Applied Biosystems, Thermo Fisher Scientific, Victoria, Australia.	Mm01545399_m1
Software and algorithms		
GraphPad Prism 9 Software	GraphPad Software 225 Franklin Street. Fl. 26 Boston, MA 02110, USA	Prism version 9.5.1

RESOURCE AVAILABILITY

Lead contact

Further information and requests for resources and reagents should be directed to and will be fulfilled by the lead contact, Dr. Vance Matthews (vance.matthews@uwa.edu.au).

Materials availability

This study did not generate new unique reagents.

Data and code availability

- Data reported in this paper will be shared by the lead contact upon request.

- This paper does not report original code.

- Any additional information required to reanalyze the data reported in this paper is available from the lead contact upon request.

EXPERIMENTAL MODEL AND STUDY PARTICIPANT DETAILS

Animal models and genotyping

In this study, we used the Kimba and Akimba mouse models. The Kimba mouse model (trVEGF029) transiently overexpresses human vascular endothelial growth factor (hVEGF) in photoreceptors and demonstrates neovascular changes associated with DR without a hyperglycemic background.[55,56] The Akita (Ins2Akita) mouse model is a naturally occurring diabetic model that carries a dominant mutation in the insulin 2 (Ins2) gene. Therefore, heterozygous Akita mice develop hyperglycemia and some features of DR.[57] By crossing Akita and Kimba mice, the Akimba (Ins2AkitaVEGF+/−) mouse model is generated, which combines the severe neovascularisation of the Kimba mouse[56] with the hyperglycemic background of the Akita mouse.[57] The Akimba mouse model displays hallmark retinal microvascular abnormalities representative of human DR and is shown to develop diabetic kidney disease.[10,18,58,59] DNA was isolated from tail clippings by using the Wizard Genomic DNA Purification Kit (Promega, Madison, WI). Genotyping of Kimba mice was carried out as described previously.[56,59] Akita mice were genotyped for the Ins2 gene as described.[60] Akimba mice were genotyped by using protocols for both Kimba and Akita mice.

Animal experiments

All experimental and animal handling activities were performed at the Harry Perkins Institute for Medical Research animal holding facility (Perth, Western Australia) in accordance with the guidelines of institutional Animal Ethics Committee. Animal ethics was approved by the Harry Perkins Institute for Medical Research Animal Ethics Committee (AE141/2019; approved: 12/02/19). Specific pathogen-free 4–5 week old male Kimba and Akimba mice were obtained from the Animal Resources Centre (Perth, WA, Australia). Only male mice were used for these studies as disease progression in females is slower and inconsistent.[18,56]

Mice were housed individually, under a 12-hour light/dark cycle, at 21 ± 2°C and were given a standard chow diet (Specialty Feeds, Glen Forrest, WA, Australia) with free access to food and drinking water. Following 7-days of acclimatization, either the SGLT2 inhibitor (EMPA; (Ark Pharma Scientific Limited, Wuhan, China); 25 mg/kg/day) or the dual SGLT1 and 2 inhibitor Sotagliflozin (SOTAG; Med Chem Express, USA; 25 mg/kg/day) or vehicle (dimethyl sulfoxide [DMSO]) was administered to each mouse via drinking

water for a period of 8 weeks.[61–65] Drinking water containing the inhibitor or vehicle was freshly prepared and replenished weekly. Urine glucose levels were measured (Keto-Diastix; Bayer, Leverkusen, Germany) before treatment to confirm the phenotype of animals and 1-week post-treatment to establish the successful development of glucosuria induced by inhibitor treatment. Body weight, consumed water volumes and food intake were measured weekly.

METHOD DETAILS

Glucose tolerance testing (GTT)

Glucose tolerance testing was carried out in non-diabetic and diabetic mice treated for 3 weeks with vehicle (DMSO), SGLT2 inhibitor Empagliflozin (EMPA) or dual SGLT1/2 inhibitor SOTAG. After fasting for ~5 hrs, mice were given an intraperitoneal glucose injection (1 g/kg; 100-200µl volumes injected) and blood glucose levels were measured via tail blood samples (~10µl) at 0, 15, 30, 45, 60, 90, 120 min using a Accu-Chek Performa blood glucose monitoring system (Roche Diagnostics, North Ryde, Australia). The Area Under the Curve (AUC) was determined using the GraphPad Prism 9 Software (Boston, USA).

Specimen collection

At the end of the experiment, mice were fasted for ~5 hours with free access to treatment water. Animals were deeply anesthetized using isoflurane inhalation. Blood samples were collected using cardiac puncture and placed on ice immediately. Fasting blood glucose was measured using the Accu-Chek Performa blood glucose monitoring system (Roche Diagnostics, North Ryde, Australia). Blood samples were centrifuged, serum collected and stored at −80°C. Brain, pancreatic and kidney (left) tissue was collected into 10% buffered paraformaldehyde for histology while the right kidney was snap frozen.

Determination of gene expression

RNA was extracted from kidney tissue using Trizol reagent (Cat#: 15596026; Invitrogen, Sydney, Australia) and cDNA synthesis was performed using the high-capacity RNA-to-cDNA kit (Cat#: 4387406; Applied Biosystems, Thermo Fisher Scientific, Scoresby VIC, Australia). Real-time PCR to determine the mRNA abundance of mouse *Sglt1* and *Hprt* (house-keeper gene) was performed using a ViiA 7 Real-Time PCR System (Applied Biosystems, Thermo Fisher Scientific, Scoresby VIC, Australia) using pre-developed TaqMan probe (FAM-labelled) and primer sets for mouse *Sglt1* (Mm00451203_m1), *Hprt* (Mm01545399_m1) and Taqman Gene Expression Master Mix (Catalog #: 4369016) from Applied Biosystems. Quantitation was conducted as previously described.[66] For each sample, Hprt C_T values were subtracted from the Sglt1 C_T values to derive a ΔC_T value. The average ΔC_T value of the vehicle treated group was then subtracted from the ΔC_T value for each sample to derive a $\Delta\Delta C_T$ value. The expression of Sglt1 relative to the vehicle treated group was then evaluated using the expression $2-\Delta\Delta C_T$.

H&E, tyrosine hydroxylase, glucagon, SGLT1 and SGLT2 immunohistochemistry

Pancreatic, kidney and brain tissue were fixed in 10% buffered paraformaldehyde for 24 hours, placed in 70% ethanol overnight, followed by wax embedding and collection of 5µm sections. Pancreatic tissue was stained with H&E. A series of sections (kidney and brain) were stained for either tyrosine hydroxylase (TH), SGLT1 or SGLT2. Sections were deparaffinised in xylene (2 × 10 minutes) and rehydrated in 100% ethanol (2 × 5 minutes), 95% ethanol (1 × 1 minute) and 70% ethanol (1 × 3 minutes). Slides were then placed under running tap water for 5 minutes. Antigen retrieval was carried out by placing tissues in pre-heated EDTA (pH 8.5; Sigma–Aldrich, Sydney, Australia) and further heating with micropower for 5 minutes. Slides were washed in PBS+0.1% Tween (2 × 5 minutes), treated with 3% H_2O_2 for 10 minutes, washed with PBS+0.1% Tween (2 × 5 minutes) and blocked with 5% Fetal Bovine Serum in PBS+0.1% Tween for 1 hour at 4°C in a humidified chamber. Glucagon was detected with a mouse anti-glucagon antibody (1:500; NB600-1506, Novus Biologicals, Melbourne, Australia), TH with a rabbit anti-tyrosine hydroxylase antibody (AB152; Merck Millipore, Australia), SGLT1 with a combination of rabbit anti-SGLT1 antibodies (1:180; Abcam, Melbourne, Australia and 1:100; Novus Biologicals, Melbourne, Australia) and SGLT2 with a combination of rabbit anti-SGLT2 (1:200; Novus Biologicals, Littleton, CO, USA) and mouse anti-SGLT2 (1:50; Santa Cruz Biotechnology, Santa Cruz, CA, USA) antibodies in 5% Fetal Bovine Serum in PBS+0.1% Tween overnight at 4°C in a humidified chamber. Antibody binding was detected with anti-rabbit (1:100, Santa Cruz Biotechnology, Sydney, NSW, Australia) or anti-mouse (1:100, Santa Cruz Biotechnology, Sydney, NSW, Australia) secondary antibodies conjugated with HRP in PBS+0.1% Tween for 1 hour. Detection was performed using Ultraview Universal DAB (3, 3'-Diaminobenzidine) detection kit

(Ventana, USA) according to the manufacturer's instructions, followed by counterstaining of nuclei with Gill's haematoxylin. Slides were washed, dehydrated, cleared and mounted using DPX (Sigma–Aldrich, Sydney, Australia).

Tissue section imaging and analysis

Images were obtained using the inverted microscopic system Nikon Eclipse Ti (Nikon, Tokyo, Japan) with a digital camera CoolSNAP HQ2 (Photometrics, Tucson, AZ, USA) linked to a computer running the image analysis software 'NIS-Elements Advanced Research' (Nikon, Tokyo, Japan). The TH staining was quantified using the free image analysis software (ImageJ 1.43j, National Institutes of Health, Bethesda, Maryland, U.S.A.) using a previously published method.[67] In brief, the image was adjusted by subtracting the background. Selection of the areas (region of interest [ROI]) containing TH positive neurons was conducted using the ROI Manager tool. The digitalized area was submitted to the plug-in "color deconvolution" using the built-in vector HDAB, where the staining of hematoxylin and diaminobenzidine (DAB) was separated into 3 different panels with hematoxylin only, DAB only and background only. The DAB only image was selected and the ROI was overlaid on the DAB only image. Using this image, the software was used to calculate the mean pixel intensity of DAB.

The mean SGLT1 or SGLT2 staining expression intensity scores were calculated in counterstained renal tissue based on a scale of 0–3 (0 = absent expression; 1 = low expression; 2 = intermediate expression; 3 = high expression). Expression scores were obtained by two independent scorers to ensure results were unbiased.

Enzyme-linked immunosorbent assays

Kidney tissues were homogenized and were analyzed for norepinephrine content (Mouse Noradrenaline NA ELISA Kit; Cusabio, Wuhan, Hubei Province, China; CSBE07870m), TNF-α and IL-6 (Elisakit.com, Melbourne, Victoria, Australia) using enzyme-linked immunosorbent assay (ELISA) kits according to the manufacturer's instructions.

QUANTIFICATION AND STATISTICAL ANALYSIS

The data was analyzed using two-tailed Student's *t-test* on GraphPad Prism 9 Software (Boston, USA). All quantitative data were expressed as mean $\pm$ Standard Error of Mean (SEM). A value of $p \leq 0.05$ was considered to be statistically significant.